PHYSICAL REVIEW B VOLUME 26, NUMBER 10 15 NOVEMBER 1982

Neutron scattering investigation of layer-bending modes in alkali-metal—graphite intercalation compounds

H. Zabel
Department of Physics and Materials Research Laboratory, University of Illinois at Urbana-Champaign, Urbana, Illinois 61801

W. A. Kamitakahara
Ames Laboratory and Department of Physics, Iowa State University, Ames, Iowa 50011

R. M. Nicklow
Solid State Division, Oak Ridge National Laboratory, Oak Ridge, Tennessee 37830
(Received 19 July 1982)

Phonon dispersion curves for low-frequency transverse modes propagating in the basal plane have been measured in the alkali-metal—graphite intercalation compounds KC_8, CsC_8, KC_{24}, and RbC_{24} by means of neutron spectroscopy. The acoustic branches show an almost quadratic dispersion relation at small q, characteristic of strongly layered materials. The optical branches of stage-1 compounds can be classified as either graphitelike branches showing dispersion, or as almost dispersionless alkali-metal-like modes. Macroscopic shear constants C_{44} and layer-bending moduli have been obtained for the intercalation compounds by analyzing the data in terms of a simple semicontinuum model. In stage-2 compounds, a dramatic softening of the shear constant by about a factor of 8 compared with pure graphite has been observed. Low-temperature results on KC_{24} indicate the opening of a frequency gap near the alkali-metal Brillouin-zone boundary, possibly due to the formation of the alkali-metal superstructure.

I. INTRODUCTION

Layered compounds with sufficiently weak interplanar interactions can have some unusual phonon characteristics, including modes that can be described as bending or rippling modes of the layers. These phonons, which are the subject of the present investigation, have propagation direction in the basal plane but displacements out of plane (sometimes designated $TA_\perp$ and $TO_\perp$). For small wave vectors q the dispersion has a characteristic $\omega \sim q^2$ dependence[1] in the absence of interlayer forces. Weak interplanar interaction induces a nonzero initial slope to the $TA_\perp$ branch, the magnitude of which is determined by the layer shear force constant C_{44} (i.e., the same elastic constant that determines the initial slope of the [001] transverse-acoustic branch). The tendency for $\omega \sim q^2$ behavior is most clearly observed in highly oriented pyrolytic graphite[2] (HOPG) and MoS_2,[3] which have especially strong-layered character and thus relatively small values of C_{44}.

In alkali-metal—graphite intercalation compounds (AGIC's) the carbon layers retain their strong intraplanar bonding, but are interleaved with intercalant layers for which both the intralayer and interlayer forces are relatively weak. The intercalation of graphite to a stage-n alkali-metal compound (the stage number n designates the number of graphite planes between adjacent intercalate planes) changes the bulk-bending modulus, as well as the layer shear modulus in a systematic way, as we shall describe below. In addition, it has been shown in previous work[4] that intercalation causes zone-folding and mode-splitting effects arising from the larger size and (generally) reduced symmetry of the unit cell.

Apart from an earlier report[5] on RbC_8, the work described here represents the first systematic inelastic neutron scattering study of transverse out-of-plane modes in stage-1 and stage-2 AGIC's. This study is a natural progression from other recent measurements of low-frequency phonons in AGIC's, such as neutron scattering studies[4] of longitudinal modes propagating normal to the planes, Raman scattering experiments[6–8] on rigid-layer

modes in KC_x and RbC_x compounds, and a neutron scattering study[5,9] of alkali in-plane modes in RbC_8. Together with earlier[10,11] Raman scattering experiments probing the high-frequency graphite-derived modes at the zone center, all the available information constitutes a fairly comprehensive picture of the lattice dynamics of AGIC's. The experiments have recently stimulated several theoretical and calculational papers on the phonon spectra of intercalated graphite. The more recent work,[12–14] which attempts to account reasonably well for all the available experiments, should especially lead to a fuller understanding of phonons in AGIC's.

II. EXPERIMENT

In this study HOPG with an initial mosaic spread of 0.2°–0.5° was used as starting material. Single crystals would, of course, have been preferable, but none of sufficient size was available to us. The phonon dispersion curves that we have measured are therefore only *averaged* dispersion relations over all directions in the basal plane. However, as demonstrated by Nicklow *et al.*[2] for pristine HOPG the graphite dispersion relation for $TA_\perp$ and $TO_\perp$ is nearly isotropic, even close to the Brillouin-zone boundary, and thus well-defined phonon dispersion curves can be measured with the use of HOPG. The same considerations apply to the present study of AGIC's, although effects due to the directional averaging and the tendency for in-plane zone-folding effects appear to give rise to more broadened and complicated neutron spectra than in pure HOPG. Another difficulty arises from the increased c-axis mosaic caused by the intercalation process, which particularly limits the determination of the $TA_\perp$ branch at small wave vectors. To keep the mosaic spread at an acceptable level the samples were intercalated very slowly with alkali metals, descending from high temperature in a two-stage tubular furnace, and thereby passing first through higher stages before reaching the desired final stage. Typical mosaic spreads obtained by this method were 1.5° for stage-2 compounds and 2°–3° for stage-1 compounds. Alkali metals from A. D. Mackay with a stated purity of 99.9% were used. The purity of stage and homogeneity of each compound was verified by x-ray and neutron elastic (00l) scans. The samples were either kept in their silica-glass intercalation vessels during the neutron measurements, or, for KC_{24} and RbC_{24}, transferred into thin-walled aluminum containers. In the latter case the samples were removed from the glass containers in a box of dry ice, transferred, and then again vacuum sealed. A sketch of the sample chamber is shown in Fig. 1.

Phonons were measured with the use of constant-$\vec{Q}$ scans on a triple-axis spectrometer at the High-Flux Isotope Reactor of Oak Ridge National Laboratory and partly at the research reactor of the National Bureau of Standards. The (002) planes of HOPG were employed as monochromator and analyzer. A fixed final energy of 3.3 THz = 13.65 meV was used throughout the experiment. Low-temperature measurements were made with a Displex closed-cycle helium-gas refrigerator.

III. RESULTS

A. Stage-1 compounds

In KC_8, RbC_8, and CsC_8 the alkali-metal atoms are centered over carbon hexagons and form in each layer a 2×2 superlattice commensurate with the adjacent graphite layers. Four equivalent interstitial sites α, β, γ, and δ are available, and the three-dimensional structure is formed by an ordered sequence $A\alpha A\beta A\gamma A\delta A\alpha\ldots$ for KC_8 and RbC_8 (Ref. 15), and $A\alpha A\beta A\gamma A\ldots$ for CsC_8 (Ref. 16). (Capital letters refer to graphite layers, and Greek letters to alkali-metal layers.) The bending modes investigated here are affected by the alkali-metal in-plane structure and by the stage number, but not, as far as we can tell, by the alkali-metal stacking sequence. Therefore, we obtain for all three compounds qualitatively similar phonon dispersion curves, as shown in Fig. 2. The RbC_8 results were obtained in an ear-

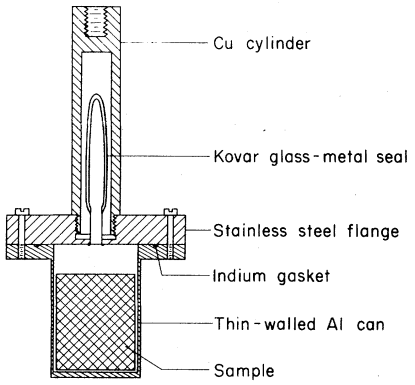

FIG. 1. Sample chamber for alkali-metal–graphite intercalation compounds used for measurements between 8.8 K and room temperature.

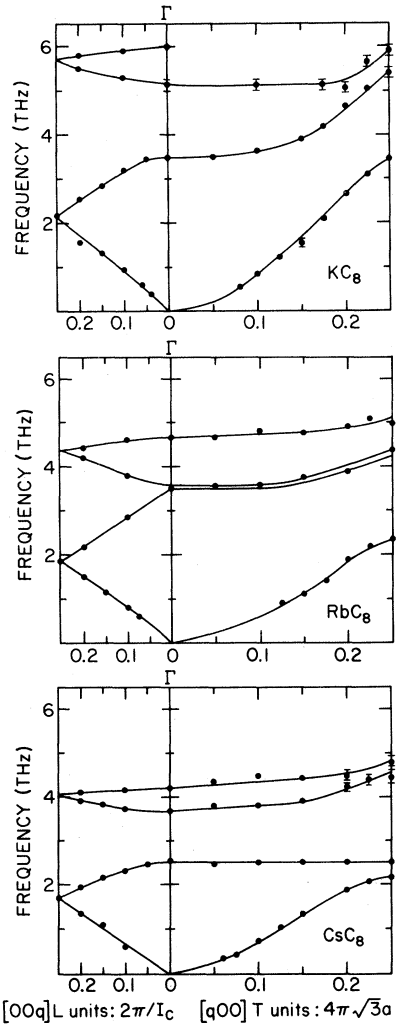

FIG. 2. Measured phonon energies of [q00] transverse modes in stage-1 alkali-metal–graphite intercalation compounds. The phonon energies of RbC_8 (Ref. 5) has been included here for completeness. In the left panel the [00q] longitudinal modes are reproduced (Refs. 4 and 17). Solid lines are guides to the eye. For details see text.

lier study[5] and are included here for the sake of completeness. In the left panels of Fig. 2 the L[001] modes of each compound are plotted from the data of Refs. 4 and 17. Note that at the Γ point L[001] and $T_\perp$[100] modes have the same symmetry, and thus the branches join together. (For convenience, we refer to the transverse modes we have observed as $T_\perp$[100] modes, although, as we have mentioned above, the measured dispersion curves are averaged over all directions in the basal plane.) It should also be noted that for each of the $T_\perp$[100] branches shown in Fig. 2, the wave-vector component q_z is constant, being either 0 (highest and lowest branches) or π/I_c (middle two branches), where I_c is the intercalate-intercalate interlayer distance along the c axis. In spite of the $\alpha\beta\lambda\delta$ stacking of KC_8 and RbC_8, the primitive unit cell spans only two intercalate layers[12] and not four, and thus the $T_\perp$[100] branches we have plotted do indeed correspond to this cell, although the q_z wave-vector unit we have chosen, $2\pi/I_c$, does not refer to the primitive cell, which would suggest the use of π/I_c. For CsC_8, which has $\alpha\beta\gamma$ stacking, the plot does not correspond to the primitive cell. However, since the dynamics are not strongly influenced by layer stacking, we have made measurements and plotted the data in the same way as for KC_8 and RbC_8 for purposes of direct comparison. Experimentally, this is done merely by fixing the value of q_z relative to an (00l) reflection at the desired value (0 or π/I_c), as shown in Fig. 3. The in-plane wave vectors in the plots of Fig. 2 are in units of $4\pi/\sqrt{3}a$, where a is the lattice constant of pristine graphite. Owing to the alkali 2×2 in-plane structure, the Brillouin-zone boundary in the [100] direction is located at $0.25(4\pi/\sqrt{3}a)$. Although, as we have explained above, there exists a directional uncertainty in the powder-averaged (hk0) plane, the phonon branches do tend to have zero slope at this wave vector.

The acoustic $T_\perp$[100] branches of all stage-1 compounds studied show a pronounced upward curvature near $q=0$, indicating the tendency for $\omega\sim q^2$ dependence at small q, characteristic of a strongly layered compound. Thus despite the fact that the alkali-metal intercalate provides bonding of mixed metallic and ionic character between graphite and

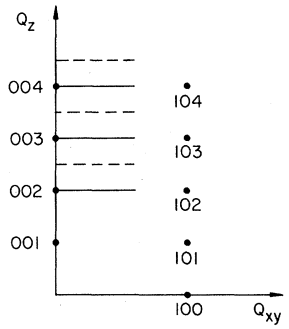

FIG. 3. Part of the reciprocal lattice of stage-1 compounds. The highest and lowest $T_\perp$[100] branches were measured along the solid horizontal lines, while the middle two branches were measured along the dashed lines. Here, the Miller indices h correspond to the graphite basal plane lattice parameter, and l to the package thickness I_c.

alkali-metal planes that is stronger than the van der Waals bonding of pristine graphite,[4] the layered character of stage-1 AGIC's is still playing a dominant role in the lattice dynamics. The optical branches are qualitatively changed by the presence of the intercalate, and can be described as dispersive graphitelike modes that are hybridized with almost dispersionless alkali-metal-like modes. This will be discussed in more detail in Sec. IV.

B. Stage-2 compounds

In contrast to stage-1 compounds, stage-2 compounds do not have well-defined three-dimensional crystal structures. At high temperatures the alkali-metal layers are disordered, exhibiting two-dimensional liquidlike structure factors.[18] At temperatures 123 and 162 K, the K and Rb intercalants in KC_{24} and RbC_{24}, respectively, undergo order-disorder phase transformations accompanied by two- to three-dimensional crossover effects[19,20] with respect to the alkali-metal—alkali-metal spatial pair-correlation function. The low-temperature alkali-metal structure and the questions of commensurability and phase homogeneity are still controversial.[21,22] Since this point is not of major importance for our results, we will not discuss it further here. However, in an average sense, it is convenient to regard the alkali layers as close-packed triangular layers with fundamental reciprocal-lattice vectors of approximately 0.43 for K and 0.40 for Rb intercalants, in units of the (100) graphite reciprocal-lattice vector length $4\pi/\sqrt{3}a=2.94$ Å^{-1}. The alkali-metal reciprocal-lattice vectors show some variation from sample to sample, probably due to slightly different in-plane concentrations. We ourselves observe 0.408 in KC_{24}, while the $\sqrt{7}\times\sqrt{7}$ structure observed by others[22] corresponds to 0.378. We believe that the dynamics of the $T_\perp$[100] modes are quite insensitive to these rather small differences.

In Fig. 4 the $TA_\perp$ and $TO_\perp$ modes of KC_{24} and RbC_{24} are shown in the right panels, again together with their adjoining L[001] modes in the left panels. Note that here only the $q_z=0$ transverse modes are recorded. In both cases the measurements have been taken at 295 K. Although in the high-temperature phase the Brillouin zone is, in principle, determined by the graphite structure only, in reality, the dynamics are strongly affected by the average in-plane alkali-metal—alkali-metal spacing. Consequently, phonon groups beyond $|q|=0.25$ are less well-defined and more difficult to interpret than those for $|q|<0.25$. Hence we have omitted data for $|q|>0.25$. In contrast, for pristine graphite[2] one can observe well-defined peaks up to $|q|=0.5$ (all q values are given in units of $4\pi/\sqrt{3}a$).

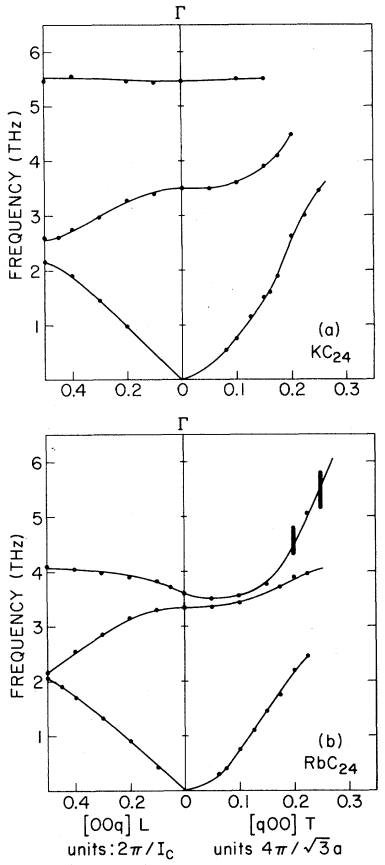

FIG. 4. Phonon energies for [q00] transverse modes in stage-2 compounds (a) KC_{24} and (b) RbC_{24}, measured at room temperature. Thick bars indicate uncertainties in the phonon energies at larger wave vectors. In the left panel the [00q] longitudinal modes of the corresponding stage-2 compounds are reproduced (Ref. 4). Solid lines are guides to the eye.

The $TA_\perp$ branches of KC_{24} and RbC_{24} again tend to show the characteristic $\omega\sim q^2$ dependence for bending modes. Unlike the case for stage-1 compounds, the $TO_\perp$ modes seem always to be of mixed graphitic and alkali-metal-like nature. This follows from examination of the eigenvectors at the Γ point in linear-chain model calculations,[23] as well as from the observation that both optical branches have significant dispersion in each of KC_{24} and RbC_{24}.

C. Low-temperature results on KC_{24}

We have made temperature-dependent measurements in order to detect the influence of the alkali-metal order-disorder transformation in stage-2 KC_{24}. One might anticipate two effects: First, the alkali-metal in-plane superlattice creates a new, smaller Brillouin zone, possibly producing mode splittings near the newly formed boundaries; second, the shear constant C_{44} might be expected to stiffen below the transition temperature. It might be noted that it is most difficult to perform ultrasonic observations[24] on AGIC's and thus to measure elastic constants directly. To our knowledge no measurements of C_{44} in an AGIC have ever been obtained by ultrasonics. Thus our neutron data constitute one of the few reliable estimates of C_{44}. The only other measure of C_{44} of which we are aware comes from analyzing the recent Raman scattering experiments[6–8] in which the $q=0$ TO[001] modes were detected in Rb and K AGIC's. The models fitted to the Raman scattering data also give C_{44} values that are much smaller than in pristine graphite, in complete accord with our neutron scattering experiment.

In Fig. 5 the phonon dispersion curves measured at 8.8 K are reproduced. At this temperature the acoustic branch shows mode splitting near $q=0.2$, corresponding to the Brillouin-zone boundary of the potassium superstructure. However, we did not observe any splitting in the optical branches at the same wave vector. A limited number of scans over this region for the acoustic branch at 110 and 150 K show that the splitting disappears with temperature not through a gradual reduction of the size of the frequency gap, but by a general broadening of the two-peak structure into a single peak. Although it is tempting to associate the gap with the formation of the alkali superlattice, further analysis and scans at more temperatures would be needed to support this interpretation.

Fig. 6 reproduces the initial slope of the acoustic branch as determined at 8.8, 150 and 295 K. For $q \lesssim 0.125$ an overall increase of about 10% is observable between the highest and lowest temperatures. Whether this rather large increase is a smooth function of temperature and whether it is due to the usual lattice anharmonicity, or instead shows a sharp onset at the transition temperature, needs to be explored in more detail in future studies.

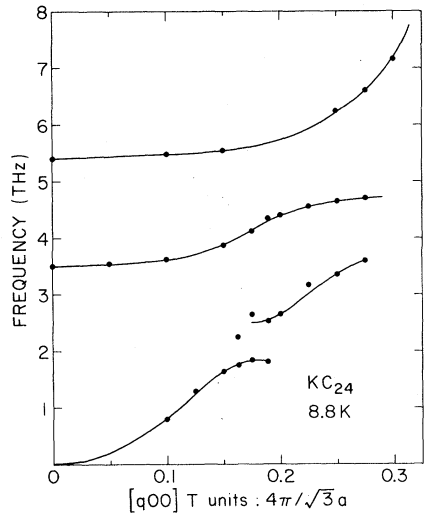

FIG. 5. [q00] transverse modes of KC_{24}, as measured at 8.8 K. Note the mode splitting in the acoustical branch, possibly due to alkali order-disorder transformation.

IV. DISCUSSION

A first description of the bending modes in graphite has been given by Komatsu.[25] In his semicontinuum model the graphite layers are considered as thin sheets of homogeneous matter stacked together into an assembly of loosely bound plates. In the following discussion we extend this model to take into account the ordered sequence of graphite and intercalate layers that occurs in AGIC's. This simple treatment of AGIC's cannot replace more detailed lattice-dynamical calculations, such as those of Horie *et al.*,[12] Leung *et al.*,[13] and Al-Jishi and Dresselhaus.[14] However, it bears the advantage of

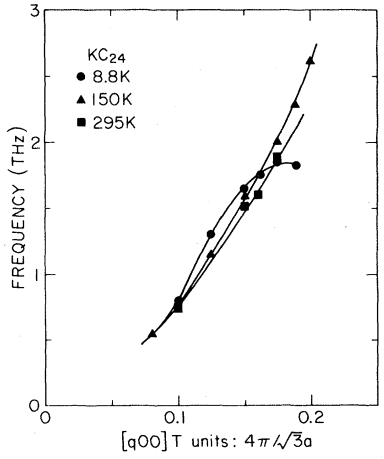

FIG. 6. Temperature dependence of the $TA_1[q00]$ branch in KC_{24}.

making transparent some important features of the bending modes in these compounds.

In general, the bending modes have wave-vector components q_z as well as q_x, q_y, thus forming a dispersion surface in reciprocal space. This is illustrated for the case of stage-1 CsC_8 in Fig. 7. The phonon branches of Fig. 2 appear here as boundary lines of the dispersion surface with either $q_z=0$ or $q_z=\pi/I_c$, as mentioned before. Figure 7 also includes a $TA_\perp$ branch taken at constant $q_z=0.33(\pi/I_c)$.

In the general case of a stage-n compound the dispersion surfaces may be described by the expression

$$\omega^2(q_{x,y},q_z)=Aq_{x,y}^2+\frac{1}{n+1}\left[\sum_{i=1}^{n+1}|a_i|B_i\right]q_{x,y}^4 +\omega_z^2(q_z)\,. \tag{1}$$

Here the constant A is proportional to the macroscopic shear constant $A=C_{44}/\rho$ and originates from the interlayer interaction. ρ is the volume density. The second term in Eq. (1) reproduces the well-known q^2 dependence of the bending modes. B_i are the bending moduli of the graphite and alkali-metal layers and the sum has to be taken over all $n+1$ graphite and alkali-metal layers within the repeat distance I_c of a stage-n compound. $|a_i|$ are normalized coefficients proportional to the eigenvectors of the [001] longitudinal modes. Finally, $\omega_z(q_z)$ are the frequencies of the [001] longitudinal modes with wave vectors q_z. It may be noted that the bending modes have a striking similarity to spin waves in ferromagnets, where the spin exchange operators J_i play the role of the bending moduli B_i.

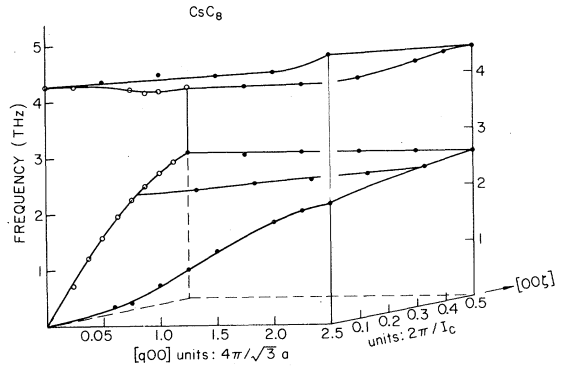

FIG. 7. Phonon dispersion surface of CsC_8 spanned by the [00q]L and $T_\perp[q00]$ phonon branches.

From Eq. (1) follow immediately some simple relationships:

(i) The $TA_\perp$ modes are characterized by $q_z=0$. Since the planes are vibrating in phase, all $|a_i|=1$, and from Eq. (1) follows Eq. (2):

$$\left[\frac{\omega^2}{q_{x,y}^2}\right]_{TA_\perp}=A+\frac{1}{n+1}q_{x,y}^2\left[\sum_{i=1}^{n+1}B_i\right]. \tag{2}$$

A plot of $(\omega^2/q_{x,y}^2)_{TA_\perp}$ vs $q_{x,y}^2$ yields the shear constant as intercept of the ordinate and the average bending modulus as slope of the linear curve. In Fig. 8 this plot is shown for most compounds studied and compared with similar data on pristine graphite.[2]

At higher $q_{x,y}$ values, deviations from the linear relation (2) are observable, indicating the validity limit of the semicontinuum ansatz (1). In order to determine the intercept and slope with acceptable accuracy, good data at small wave vectors are needed. However, as mentioned before, this is the most troublesome wave-vector region because of the rather large mosaic spread inherent to low-stage graphite intercalation compounds. Nevertheless, we were able to deduce from the data the elastic constants listed in Table I. Compared to pristine graphite the shear constant C_{44} in stage-1 compounds is smaller by about 25% and in stage-2 compounds by a factor of 5–10. Thus, especially for stage-2 compounds, intercalation of alkali-metal layers

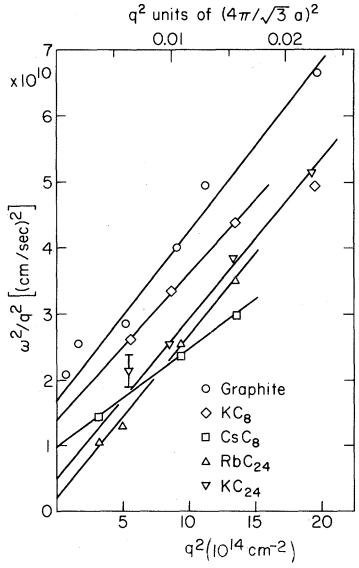

FIG. 8. Phonon frequency of $TA_\perp[q00]$ modes plotted as ω^2/q^2 vs q^2 for pure graphite and alkali-metal–graphite intercalation compounds. The solid lines are least-square fits to the experimental points.

TABLE I. Elastic moduli for shear (C_{44}) and bending (B) derived, respectively, from the intercepts A and slopes D of the lines in Fig. 8. Also see Eq. (2) and related text.

	A (10^{10} cm^2/sec^2)	ρ (g/cm^3)[a]	C_{44} (10^{10} dyn/cm^2)	B (10^{-5} cm^4/sec^2)[b]
Graphite	1.7±0.2	2.26	3.84±0.4	2.55±0.15
KC_8	1.4±0.1	2.012	2.82±0.2	1.66±0.1
CsC_8	1.0±0.05	3.07	3.07±0.15	1.48±0.05
RbC_{24}	0.20±0.1	2.19	0.44±0.2	2.48±0.1
KC_{24}	0.45	1.98	0.89±0.2	2.45±0.15

[a]Reference 4.

[b]$B=\frac{1}{n+1}\sum_{1=1}^{n+1} B_i$.

causes a dramatic softening of the macroscopic shear constant. This observation is in very good agreement with recent Raman scattering results on rigid-layer shear modes of K and Rb AGIC's.[6–8] Also, in the stage-1 acceptor compound $FeCl_3$-intercalated graphite some softening of the shear constant has been observed.[24]

From the Raman scattering results[6–8] we know that the soft shear constant in stage-2 compounds is due to a very weak alkali-metal–graphite layer shearing interaction. Assuming nearest-neighbor interlayer interaction only, the interlayer shear force constants obtained from the Raman shifts are related to the macroscopic shear constant by

$$\frac{1}{C_{44}}=\frac{c_0}{f_0}+\frac{c_1}{f_1}\ . \tag{3}$$

Here c_0 is the interior graphite layer spacing, c_1 the graphite–alkali-metal–graphite package thickness, f_0 the shear force constant between graphite planes, and f_1 the shear force constant between alkali-metal and graphite planes. With the use of Eq. (3) we find reasonable agreement between the Raman scattering results and the macroscopic shear constant C_{44} derived from the $TA_\perp$ branch. The bending moduli of AGIC's, also listed in Table I, appear somewhat smaller than in pure graphite, although the effect is not as dramatic as for the shear constant.

(ii) At the zone boundary of stage-1 compounds ($q_z=\pi/I_c$), $|a_M|=1$ and $|a_m|=0$ for the acoustic branch, and $|a_M|=0$ and $|a_m|=1$ for the optical branch. m and M refer to the smaller or larger area-mass density of the planes, respectively. Thus at the zone boundary the bending modes of graphite and alkali-metal layers are decoupled. For instance, the zone-boundary $TA_\perp$ mode of CsC_8 is determined by the alkali-metal vibration only, since the alkali-metal layer has the larger area-mass density, whereas the zone-boundary $TO_\perp$ mode is due solely to the graphite vibration. Similar arguments apply for the other stage-1 AGIC's, except that the role of the zone-boundary $TA_\perp$ and $TO_\perp$ modes is reversed: the lower branch being graphitelike and the upper alkali-metal-like.

The alkali-metal-like branches are almost flat, indicating that the bending modulus of the alkali-metal layers is essentially zero. In the case of KC_8 and RbC_8, and at larger wave vectors $q_{x,y}$, the flat $TO_\perp$ branch has the tendency to cross the graphitelike $TA_\perp$ dispersion curve, leading to a mode splitting and exchange of their character thereafter. For the zone-center ($q_z=0$)$TO_\perp$ branch $|a_M|=|a_M|=1$ again, and apart from the term $\omega^2(q_z=0)$, this branch represents an image of the acoustical branch.

(iii) In the case of the stage-2 compounds KC_{24} and RbC_{24}, the $TO_\perp$ modes are of mixed graphite and alkali-metal character. Nonetheless, the first zone-center optical mode is predominantly determined by the large amplitude of the graphite layers, whereas the second zone-center optical mode is almost entirely due to the alkali-metal-layer vibration. This effect is more pronounced for the lighter potassium layers than for the rubidium layers. As in stage-1 compounds a crossover effect from alkali-metal-like to graphitelike dispersion and vice versa can be observed when both branches tend to cross. (Compare Figs. 4 and 5.)

Apart from this qualitative discussion of the $TA_\perp$ and $TO_\perp$ modes, the lattice-dynamical calculation of Al-Jishi and Dresselhaus[14] gives a rather good agreement with our data on RbC_{24}. Their most complete lattice-dynamical calculation on AGIC's to date requires only some refinements to obtain improved fits for the other compounds too. There is every reason to expect that eventually all the known features of the lattice dynamics of AGIC's, including shear modes,[6–8] in-plane intercalate modes,[5–9]

bending modes, and perturbed high-frequency modes,[10-11] can be reasonably accounted for within a unified lattice-dynamical model.

V. SUMMARY

We have measured and analyzed the layer bending modes in the layered structures of stage-1 and -2 AGIC's. We found that the shear constants are dramatically softened in stage-2 compounds, but are already smaller in stage-1 compounds than in pure graphite. The bending modulus of alkali-metal layers is almost zero, which is not completely unexpected. We have observed crossover effects from alkalilike to graphitelike optical-phonon branches, and a mode splitting in the acoustic branch of stage-2 KC_{24}, which may be related to the alkali-metal order-disorder transformation.

ACKNOWLEDGMENTS

We wish especially to thank A. W. Moore of Union Carbide Corporation, who donated the large HOPG samples that made these measurements possible. We also wish to thank G. Dresselhaus and R. Al-Jishi for useful conversations, and for generously communicating to us results of their theoretical studies prior to publication. The Ames Laboratory and Oak Ridge National Laboratory are, respectively, operated by Iowa State University and Union Carbide Corporation under Contract Nos. W-7405-Eng-82 and W-7405-Eng-26 with the U.S. Department of Energy (USDOE). One of us (H.Z.) was supported by USDOE Contract No. DE-AC02-76ER01198, within the Materials Research Laboratory of the University of Illinois, Urbana-Champaign. All support for this work was managed by the Office of Basic Energy Sciences, USDOE.

[1]Lord Rayleigh, *Theory of Sound* (MacMillan, London, 1894), Vol. 1, p. 352; L. D. Landau and E. M. Lifshitz, *Theory of Elasticity* (Pergamon, New York, 1970).
[2]R. M. Nicklow, N. Wakabayashi, and H. G. Smith, Phys. Rev. B 5, 4951 (1972).
[3]N. Wakabayashi, H. G. Smith, and R. M. Nicklow, Phys. Rev. B 12, 659 (1975).
[4]H. Zabel and A. Magerl, Phys. Rev. B 25, 2461 (1982).
[5]W. A. Kamitakahara, N. Wada, and S. A. Solin, J. Phys. (Paris) Colloq. 42, C6-311 (1981); Solid State Commun. (in press).
[6]N. Wada, M. V. Klein, and H. Zable, J. Phys. (Paris) Colloq. 42, C6-350 (1981).
[7]P. C. Eklund, J. Giergiel, and P. Boolchand, in *Physics of Intercalation Compounds,* Vol. 38 of *Springer Series in Solid State Sciences,* edited by L. Pietronero and E. Tosatti (Springer, Berlin, 1981).
[8]J. Giergiel, P. C. Eklund, R. Al-Jishi, and G. Dresselhaus, Phys. Rev. B (in press).
[9]W. A. Kamitakahara, H. Zabel, and R. M. Nicklow (unpublished).
[10]P. C. Eklund, G. Dresselhaus, M. S. Dresselhaus, and J. E. Fischer, Phys. Rev. B 21, 4705 (1980).
[11]R. J. Nemanich, S. A. Solin, and D. Guérard, Phys. Rev. B 16, 2965 (1977).
[12]C. Horie, M. Maeda, and Y. Kuramoto, Physica (Utrecht) 99, 430 (1980).
[13]S. Y. Leung, G. Dresselhaus, and M. S. Dresselhaus, Phys. Rev. B 24, 6083 (1981).
[14]R. Al-Jishi and G. Dresselhaus, Phys. Rev. B 26, 4514 (1982).
[15]P. Lagrange, D. Guérard, M. El Makrini, and A. Hérold, C. R. Acad. Sci., Ser. C 287, 179 (1978).
[16]D. E. Nixon and G. S. Parry, Br. J. Appl. Phys. Ser. 2 1, 291 (1968).
[17]W. D. Ellenson, D. Semmingson, D. Guérard, D. G. Onn, and J. E. Fischer, Mater. Sci. Eng. 31, 137 (1977).
[18]G. S. Parry and D. W. Nixon, Nature (London) 216, 909 (1967).
[19]H. Zabel, S. C. Moss, N. Caswell, and S. A. Solin, Phys. Rev. Lett. 43, 2022 (1979).
[20]M. Suzuki, H. Ikeda, H. Suematsu, Y. Endoh, H. Shiba, and M. T. Hutchings, J. Phys. Soc. Jpn. 49, 671 (1980).
[21]M. Mori, S. C. Moss, Y. M. Jan, and H. Zabel, Phys. Rev. B 25, 1287 (1982).
[22]R. Clarke, J. N. Gray, H. Homma, and M. J. Winokur, Phys. Rev. Lett. 47, 1407 (1981).
[23]A. Magerl and H. Zabel (unpublished).
[24]D. M. Hwang, B. F. O'Donnell, and A. Y. Wu, in *Physics of Intercalation Compounds,* Vol. 38 of the *Springer Series in Solid State Sciences,* edited by L. Pietronero and E. Tosatti (Springer, Berlin, 1981).
[25]K. Komatsu, J. Phys. Soc. Jpn. 10, 346 (1955).